Journal of Building Engineering 64 (2023) 105620

Contents lists available at ScienceDirect

Journal of Building Engineering

journal homepage: www.elsevier.com/locate/jobe

Reliability assessment of ground granulated blast furnace slag/ cow bone ash- based geopolymer concrete

John Oluwafemi [a,*], Olatokunbo Ofuyatan [a], Adeola Adedeji [b], Deborah Bankole [c], Lazarus Justin [a]

[a] Department of Civil Engineering, Covenant University, Ota, Ogun State, Nigeria
[b] Department of Civil Engineering, Ilorin, Kwara state, Nigeria
[c] Department of Industrial Chemistry, Landmark University, Omu-Aran, Kwara state, Nigeria

ARTICLE INFO

Keywords:
Reliability
Geopolymer concrete
Conventional concrete
Service life
Wastes
Mechanical properties

ABSTRACT

This study focused on the reliability assessment of ground-granulated blast furnace slag (GGBS) and cow bone ash (CBA) based geopolymer concrete (GPC). To produce the GPC, sodium silicate (Na_2SiO_3) was mixed with sodium hydroxide of 12M at a 2.5:1 ratio and used as the alkaline activator. The mechanical properties of the GPC were examined at 7, 14, 28, 56, and 90 days of ambient curing. Microstructural analyses were also carried out to investigate the microstructural properties that influence the mechanical performance of the GPC. Following these, a reliability assessment was carried out to establish the reliability of GPC using the constant failure model method. The results of the mechanical tests showed that GPC with GGBS composition that is $\geq$ 60% and CBA that is $\leq$ 40% performed better than the conventional concrete. At 28 days of curing, the GPC optimum mix attained a compressive strength of 40.13 MPa against 33.14 MPa attained by the conventional concrete. Also, the reliability analyses established that GPC mixes with GGBS composition that is $\geq$ 60% and CBA that is $\leq$ 40% are reliable up to the expected 50 years of service for structures. Hence, GPC is reliable as well as conventional concrete.

1. Introduction

Concrete is the most widely used construction material globally. This makes concrete structures one of the most existing structures in many countries of the world. Annually, about thirty billion tons of concrete is produced globally, which is expected to have an uptrend with time [1]. This is no surprise given the global rate of population growth and urbanization. While cement is the major component in concrete production, it contributes about 7% of the total carbon dioxide (CO_2) released into the atmosphere yearly [2]. The release of CO_2 to the atmosphere from cement production is rather on the increase on daily basis due to the continuous demand for cement in the construction of concrete structures. The high carbon footprint concern of concrete has led to the discovery of novel concrete such as geopolymer concrete (GPC), which is said to stand out as a sustainable concrete among other concrete types due to its zero cement usage [3].

Geopolymer concrete (GPC) is produced through the utilization of silica and alumina-rich waste materials such as rice husk ash (RHA), slag, metakaolin, and fly ash [4–6]. The alumino-silica content in the source materials reacts with alkaline activators to form geopolymer binders [7–11]. Sequence to the elimination of cement usage in geopolymer concrete, CO_2 emission and waste deposit in

* Corresponding author.
E-mail address: john.oluwafemi@covenantuniversity.edu.ng (J. Oluwafemi).

https://doi.org/10.1016/j.jobe.2022.105620
Received 19 August 2022; Received in revised form 15 November 2022; Accepted 24 November 2022
Available online 28 November 2022

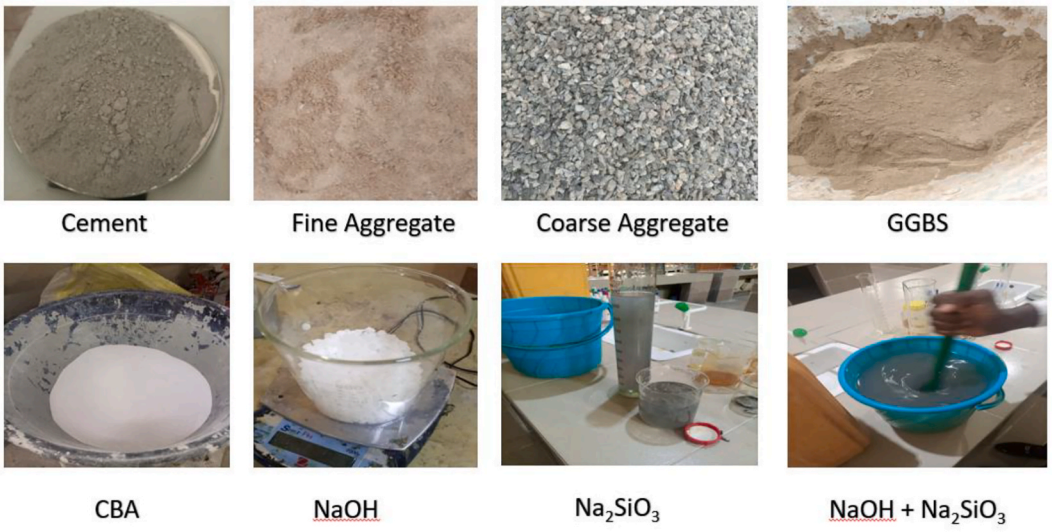

Fig. 1. Materials used.

the society is substantially reduced [12,13]. In recent times, the use of GPC in the construction industry has increased due to the necessity to combat air pollution and global warming [14]. Even though GPC has not gained global popularity and implementation in the construction industry, it has been used for the construction of structures such as reinforced box culverts, foundations, bridges, pavements, pipes, and precast structural members around the world [15]. Some other structures such as the Brisbane wellcamp airport [16], a 20-storey residential building, Lipetsk [17], a 9-storey residential building in Ukraine [18], and a residential building [19] were constructed using GPC.

One of the recent studies on GPC is the research of Zhang et al. [20], where the effect of different molar ratios of SiO_2/Na_2O on the mechanical properties of metakaolin-fly ash-based alkali-activated mortar was investigated. The findings showed that SiO_2/Na_2O of 1.2 demonstrated the highest flexural, split and compressive strength, as well as elastic modulus. Zhang et al. [21] also investigated the effect of polyvinyl alcohol fiber reinforcement and elevated temperature on metakaolin-fly ash-based geopolymer mortar. The findings from this study showed that an increase in temperature exposure from 25 °C to 200 °C improved the mechanical properties of the geopolymer mortal as well as the presence of polyvinyl alcohol fiber reinforcement. Jayarajan & Arivalagan [22] also incorporated steel fibres in the development of GPC using GGBS and fly ash as source materials. The curing of the samples was observed between 3 and 28 days. The findings of the study also confirm that the mechanical properties of GPC are improved with an increase in curing days, GGBS and steel fibre composition.

Generally, geopolymer concrete has been established to have better mechanical performance [23], lower CO_2 emission [24], better fire resistance [25], higher acid attack resistance [26], and less prone to freeze and thaw cycle [27] when compared to the conventional concrete. Nevertheless, a major gap that has been identified in the production of GPC is that there is no design standard for its production [28,29] as researchers have used design standards for conventional concrete as a reference in the past. Meanwhile, to establish a design code of practice, reliability assessment is a vital and basic requirement [30]. Presently, the reliability of conventional concrete has been established across past studies [31–35] but there is no footprint on the reliability of GPC for satisfactory performance during its service life. To this end, the aim of this study is to carry out a reliability assessment of ground granulated blast furnace slag and cow bone ash-based geopolymer concrete as a step toward actualizing a design code of practice for GPC. Before now, cow bone ash (CBA) has been successfully utilized in concrete production but not in GPC. Its utilization in GPC production in this study is hinged on its availability as animal waste in Nigerian abattoirs (more than a million tons annual generation) [36]; its chemical composition that is similar to that of cement [19,23]; reports from its usage in concrete which show satisfactory mechanical performance and improved resistance to acid attack [36–47]. Hence, the utilization of CBA in this study contributes toward the actualization of sustainable development goals. Therefore, this study developed GPC using CBA and GGBS as source materials, and the reliability assessment of the same was carried out using the constant failure rate model.

2. Materials and methods

2.1. Materials

The wastes utilized in this study as source materials are ground granulated blast furnace slag (GGBS) and Cow Bone Ash (CBA) while the alkaline activators are sodium silicate (Na_2SiO_3) and sodium hydroxide (NaOH). River sands and granites were utilized as fine and coarse aggregates respectively. Portland limestone cement of grade 42.5 was used to produce conventional concrete. MasterRheobuild 858 was used as superplasticizers. The GGBS was obtained from African Refractory and Allied Products Limited which is located at Km 46, Ikorodu Shagamu road, Ogijo, Ogun State in Nigeria (6°32′00.2″ N 304′42.6″ E) while the Cow bones were obtained from Sokoto slaughter in Nigeria (13°04′27.5″ N 5°13′33.1″ E). The GGBS was crushed with an abrasion machine and sieved with a 75

Table 1
Oxides composition of materials.

Sample	SiO_2	Al_2O_3	Fe_2O_3	CaO	MgO	SO_3	K_2O	Na_2O	LOI
OPC	18.78	4.44	3.25	69.53	1.84	1.12	0.16	0	1.85
GGBS	32.95	10.12	1.52	45.66	7.78	0.73	0.23	0.13	1.02
CBA	14.65	13.96	2.94	62.24	1.95	0.95	0.93	0.75	1.65

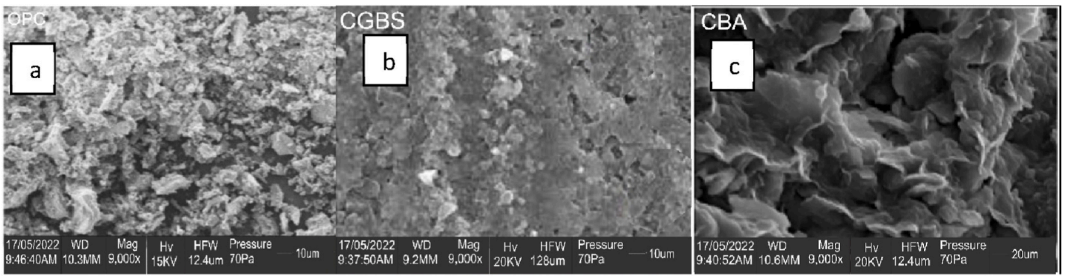

Fig. 2. SEM Images of materials (a) Cement (b) GGBS (c) CBA.

Table 2
Particle size distribution of coarse aggregates.

S/N	Sieve Size (mm)	Soil Retained (g)	Cumulative retained (g)	% Mass Retained	% Passing
1	25.00	0.00	0.00	0.00	100.00
2	19.00	21.00	21.00	2.10	97.90
3	12.50	427.00	448.00	44.84	55.16
4	9.50	282.00	730.00	73.07	26.93
5	6.30	219.00	949.00	94.99	5.01
6	4.75	39.00	988.00	98.90	1.10
7	Pan	11.00	999.00		

Table 3
Particle size distribution of fine aggregates.

S/N	Sieve Size (mm)	Soil Retained (g)	Cummulative retained (g)	% Mass Retained	% Passing	BS Limits
1	4.75	5	5	1	99	89–100
2	2.36	15	20	4	96	60–100
3	1	161	181	36.2	63.8	30–100
4	0.6	104	285	57	43	15–100
5	0.3	133.5	418.5	83.7	16.3	5–70
6	0.15	60.5	479	95.8	4.2	0–15
7	0.075	18	497	99.4	0.6	NA
8	Pan	3	500			

μm sieve opening. The CBA was also sun-dried and subjected to controlled burning at 600 °C [36]. The bones were crushed using an abrasion machine and further sieved with a 75 μm sieve opening. The liquid sodium silicate was obtained from African Fertilizer and Chemicals Limited plant located in Agbara in Ogun State in Nigeria (6°32′00.2″ N 3°04′42.6″ E) while the sodium hydroxide pellets were purchased from Allschoollabs that is located in 104 Western Avenue, Ojuelegba, Lagos State in Nigeria (6°30′34.2″ N 3°21′45.6″ E). The superplasticizer was provided by Master Builders Construction Chemicals Solutions Nigeria Limited which is located at 1, Ilupeju Bypass, Ilupeju, Lagos in Nigeria (6°32′41.4″ N 3°21′26.9″ E). The fine and the coarse aggregates were obtained from local suppliers within the locality of Ota, Ogun State, Nigeria. The fine aggregates that were used passed through a 4.75 mm sieve opening while the coarse aggregates passed through a 19 mm sieve opening. The properties of the fine and coarse aggregates were examined following BS EN 12620 [47]. The specific gravity of the cement, GGBS, CBA, fine aggregate, and coarse aggregate were 3.12, 3.0, 2.58, 2.66, and 2.75 respectively. The water absorption values of the fine and the coarse aggregates were 1.6% and 0.98% respectively. The fineness of cement, CBA, and GGBS was 2%, 1.4%, and 1.5% respectively. Fig. 1 and Table 1 show the pictures of the materials used and the chemical compositions of the source materials used while Fig. 2 shows the SEM images of the source materials. The oxide compositions of the source materials are similar to the chemical composition of materials used by other researchers in previous studies [23,44,46,48–53]. Similarly, the SEM images of the source materials produced at 9000x magnification are shown in Fig. 2. The SEM image of cement shown in Fig. 2a revealed a high specific surface area and fineness, which can cause high reactivity and density [54]. The image of the GGBS shown in Fig. 2b also revealed dense, and irregular-shaped particles [44,55], and Fig. 2c shows the SEM image

Table 4
Mix design of M30 GPC.

Mix ID	GGBS (kg/m^3)	CBA (kg/m^3)	OPC (kg/m^3)	FA (kg/m^3)	CA (kg/m^3)	Water (kg/m^3)	SH (kg/m^3)	SS (kg/m^3)
Control	0	0	466.67	681.56	1034.73	210	0	0
G100C0	466.67	0	0	681.56	1034.73	–	60	150
G80C20	373.34	93.33	0	681.56	1034.73	–	60	150
G60C40	280	186.67	0	681.56	1034.73	32.67	60	150
G40C60	186.67	280	0	681.56	1034.73	65.33	60	150
G20C80	93.33	373.34	0	681.56	1034.73	98.01	60	150
G0C100	0	466.67	0	681.56	1034.73	98.01	60	150

FA – Fine Aggregate; CA – Coarse Aggregate; SH- Sodium Hydroxide; SS – Sodium Silicate; OPC – Ordinary Portland Cement; GGBS – Ground Granulated Blast Furnace Slag; CBA – Cow Bone Ash; w/b - water to binder ratio = 0.45; b/agg - binder to aggregate ratio = 0.27.

Fig. 3. Experimental procedures and tests.

of CBA to be porous, less dense, and irregular and flaky-shaped [54].

The fine aggregates passed through a 4.75 mm sieve opening while the coarse aggregate passed through a 25 mm sieve opening. Tables 2 and 3 present the particle size distribution of the fine and coarse aggregates respectively.

The sizes of the fine aggregates and the coarse aggregates are within the limits specified in BS EN 882 [56]. The sodium silicate had specific gravity, Na_2O, SiO_2, Na_2O: SiO_2, and total solids of 1.56, 15.40, 30.81, 1:2.00, and 46.21%, respectively. The chemical composition of the Na_2SiO_3 meets the recommendation of Patankar et al. [45].

2.2. Mix design

The mix design adopted for this study is shown in Table 4. The mix was designed to attain a target strength of 30 N/mm^2 at 28 days of curing. Presently, GPC has no design standard to guide production [29,57]. Hence, BS DOE [38] was followed as in previous studies.

The water/activator to cement/binder ratio was fixed at 0.45 while Na_2SiO_3 to NaOH ratio was fixed at 2.5. The superplasticizer was also fixed at 1.5% of the binder content for the control samples and 7% for the GPC samples due to the high water demand of the mixes [58].

2.3. Preparation of alkaline activator

Sodium hydroxide solution of 12 M, being the optimum concentration for geopolymer concrete [39], was prepared following standard laboratory procedures. A total of 480 g of sodium hydroxide pellets was dissolved in water. More water was then added to the sodium hydroxide solution till it reached 1 L. The sodium hydroxide solution was prepared 24 h before the casting of the GPC. The 24 h rest period was to allow the sodium hydroxide solution to give off its heat [29,57]. Sodium silicate was mixed with sodium hydroxide after 24 h in a ratio of 2.5:1.

2.4. Mixing, casting, and experimental tests

The mixing of the GPC was done manually, nevertheless, appropriately and rigorously to attain homogeneity. The batching was done by weight method. The proportioning of the source materials followed the recommendations from previous studies [39,48,59–67]. CBA substitution interval was used as recommended by Olutaiwo et al. [68]. Slump tests and compaction factor tests were

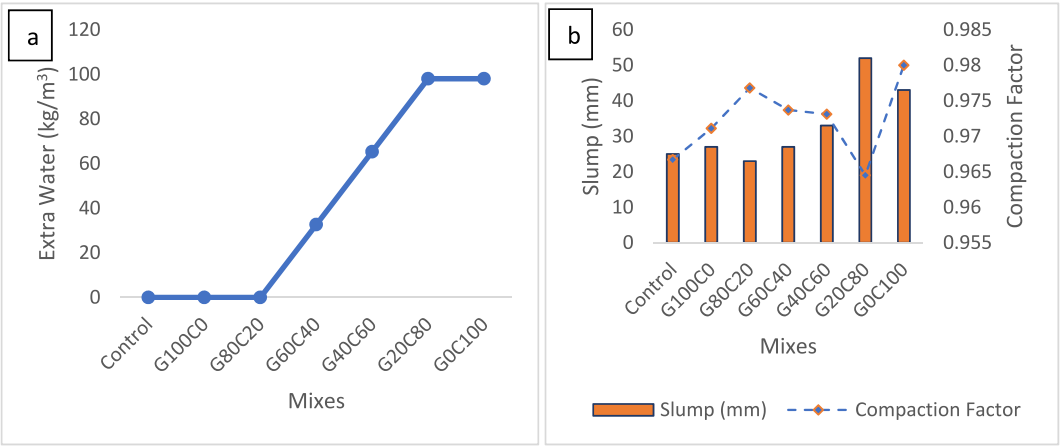

Fig. 4. Fresh properties (a) extra water demand (b) slump and compaction factor.

carried out on the fresh GPC and the conventional concrete following BS EN 12350–2 [69] and BS EN 12350–4 [70] respectively. The geopolymer concrete was cast following British Standard 1881-Part 125 [71] and British Standard EN 12390–2 [72]. The fresh geopolymer concrete was filled into the mold in 3 layers and each layer was compacted 25 times with a tamping rod. The mold was properly vibrated to ensure proper compaction and void removal. The samples were demolded after 24 h and cured for 7, 14, 28, 56, and 90 days in ambient curing temperatures that ranged between 20 °C and 22 °C. At 28 days of curing, density tests were carried out on the hardened cubes (150 mm × 150 mm x 150 mm) following BS EN 12390–7 [73]. The hardened cubes and cylinders (150 mm diameter x 300 mm) were subjected to compressive and split tensile strength tests at 7, 14, 28, 56, and 90 days using a compressive test machine of 2000 kN capacity. A flexural strength test machine was also used to test for the flexural strength of the hardened beams (100 mm × 100 mm x 500 mm). The compressive strength test, split tensile test and flexural strength test of the samples were all carried out following BS EN 12390–3 [74], BS EN 12390–6 [75], and BS EN 12390–5 [76] respectively. A total of 105 cubes, beams, and cylinders were cast and crushed. Fig. 3 shows pictures of experimental procedures and tests carried out in this study. To identify the chemical composition of the source materials and the surface morphology of the hardened samples, X-ray fluorescence equipment (Phillps PW-1800) and scanning electron microscope equipment (JOEL-JSM 7600F) were used respectively.

2.5. Reliability analysis

The probability of survival of the GPC was established using Eq. (1).

$$F(t) = \Pr\{T < t\} \tag{1}$$

where T is assumed to be the continuous random variable with a condition that t has occurred.

The cumulative density function of the survival function relates to a convenient equation to work with as expressed in Eq. (2).

$$S(t) = \Pr\{T \geq t\} = 1 - F(t) = \int_t^{\infty} f(x)dx \tag{2}$$

The hazard function was further established using Eq. (3).

$$\lambda(t) = \lim_{dt \to 0} \frac{\Pr\{t \leq T < t + dt | T \geq t\}}{dt} \tag{3}$$

The reliability index was further established using the constant failure rate reliability model [55,77]. The probability density function of the distribution is defined in Eq. (4).

$$f(t) = \lambda e^{-\lambda t} \tag{4}$$

where λ is the failure rate and t represents time (years).

The reliability function is defined in Eq (5).

$$\text{Reliability} = e^{-\lambda t} \tag{5}$$

3. Results and discussion

3.1. Properties of materials

3.1.1. Fresh properties

Fig. 4 presents the fresh properties of the mixes used in this study. The extra water, slump, and compaction factor values are

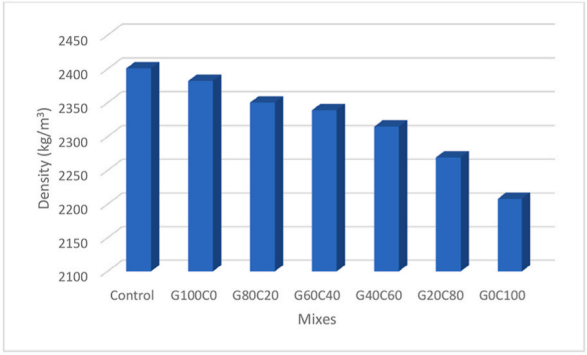

Fig. 5. Density of the hardened samples.

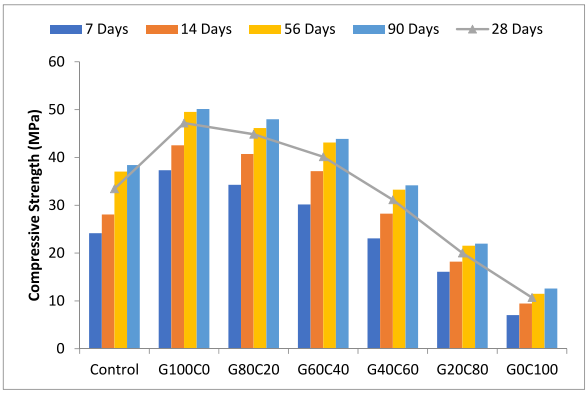

Fig. 6. Compressive strength of the hardened cubes.

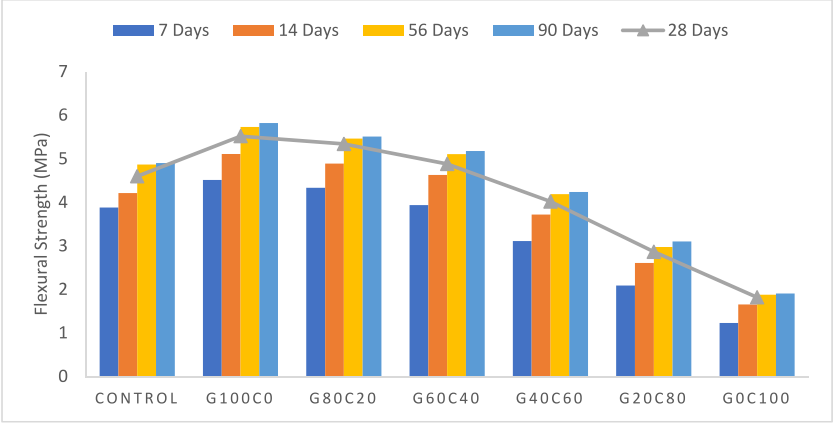

Fig. 7. Flexural strength of the hardened beams.

illustrated in Fig. 4a and b respectively.

The demand for extra water was observed to increase as the CBA composition in the mixes increased. Similarly, the slump of the mixes reduced as the CBA composition increased and it increased as the GGBS composition increased. The demand of the mixes with higher CBA content for more water is due to the higher fineness and water absorption of CBA over GGBS [44,78]. This study is further supported by the study of Getahun & Bewket [78] where CBA was used to replace cement in concrete production. The mixes with high CBA composition required much water and hence a lower slump. A similar trend was observed in the study of Olutaiwo et al. [44] and Lamidi et al. [79]. The slump values of the GPC mixes G100C0, G80C20, G60C40, G40C60, G20C80, and G0C100 were 22 mm, 18 mm, 24 mm, 28 mm, 45 mm, and 36 mm respectively while the GPC mixes had compaction factor values of 0.976, 0.971, 0,974, 0.9791, 0.9891 and 0.9841. The linear relationship observed between slump and compactor factor test results in this study agrees with the

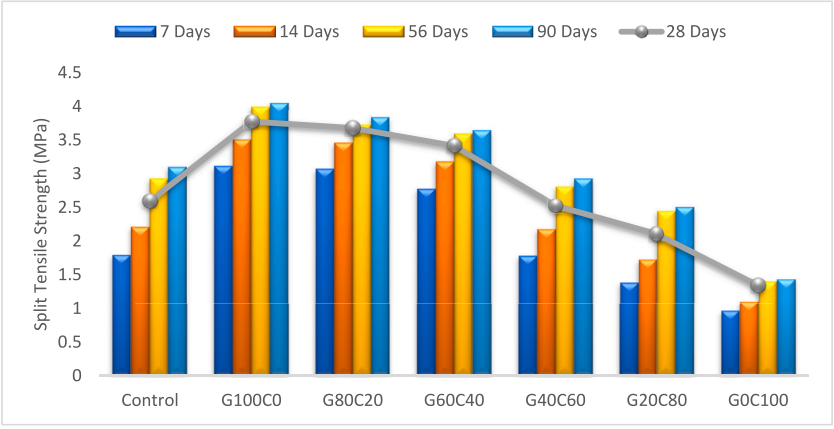

Fig. 8. Split tensile strength of the hardened cylinder samples.

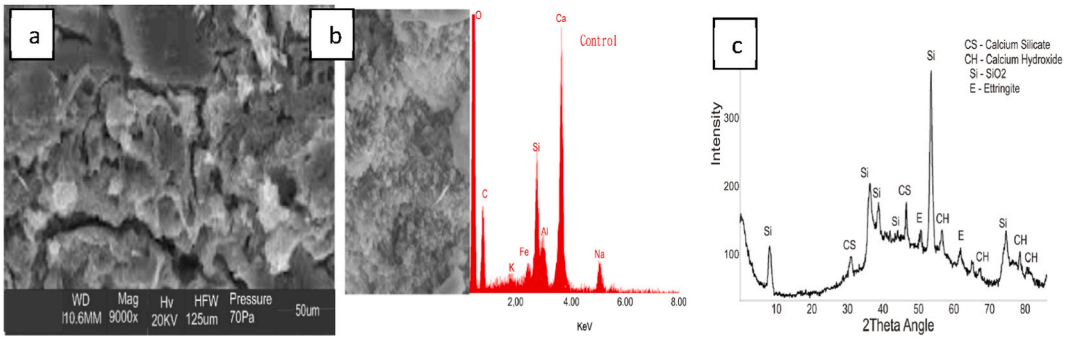

Fig. 9. Microstructural properties of control sample G60C40 (a) SEM (b) EDX (c) XRD

trend observed in the study of Zuaiter et al. [80] where slump and compactor factor test results of slag and fly ash-based GPC were compared.

3.2. *Hardened properties*

The results obtained from carrying out density tests, and compressive, flexural, and split tensile strength tests on the hardened samples are illustrated in Figs. 5–8. The density of the hardened cubes reported in Fig. 5 shows that the density of the GPC is lower than that of the conventional concrete. Also, the densities of the GPC samples with high GGBS composition were higher than the densities of the samples with high CBA composition. This is because the specific gravity of GGBS is higher than the specific gravity of CBA.

From Figs. 6–8, the strength of the geopolymer concrete increased with an increase in the composition of GGBS [81] and it decreased with an increase in the composition of CBA [44]. The observation on the effect of GGBS on the mechanical properties of the GPC is in agreement with the results from the study of Kumar, Pankar, Manish & Santhi [64] where the strength of GGBS-based GPC increased with an increase in GGBS composition. Similarly, an improvement in mechanical properties was also observed with an increase in GGBS composition in the study of Shobha & Hadole [82]. The strength of the geopolymer concrete also increased with an increase in the curing age. This is in alignment with the observation of mechanical properties trend in the study of Rao & Kumar [83] where GGBS-based GPC was developed. The strength of the GPC also increased with an increase in the curing ages of the GPC. This trend also agrees with the report of Rajini & Shashidhar [65] where the strength of the GPC was investigated for 90 days. The rate of strength development decreased as the CBA composition increased and it also decreased at subsequent curing days after 28 days of curing. This is because geopolymerization process of geopolymer concrete is almost complete at 28 days of ambient curing and 7 days of heat curing [84]. The reduction in strength rate observed in this study is in agreement with the results reported in the study of Rajini & Shashidhar [65]. The effect of GGBS and CBA composition is valid for compressive strength, flexural strength, and split tensile strength. The increase in GGBS composition that caused the increase in strength is due to increased reactive activities of GGBS, which facilitated the formation of sodium alumino-silicate hydrate (N-A-S-H) gel and calcium alumino-silicate hydrate (C-A-S-H) gel and hence, accelerated geopolymeric reaction [25]. Meanwhile, in line with this study, the trend observed with mechanical properties of the GPC when the composition of CBA increased is similar to the trend observed in previous studies where the composition of other source materials increased against the composition of GPC [64]. The average compressive strength of the geopolymer concrete cubes illustrated in Fig. 6 attained 33.44 MPa, 47.19 MPa, 44.85 MPa, 40.13 MPa, 31.13 MPa, 20.00 MPa, and 10.68 MPa for Control, G100C0, G80C20, G60C40, G40C60, G20C80, and G0C100 respectively at 28 days of curing. Hence, mixes with 60% GGBS

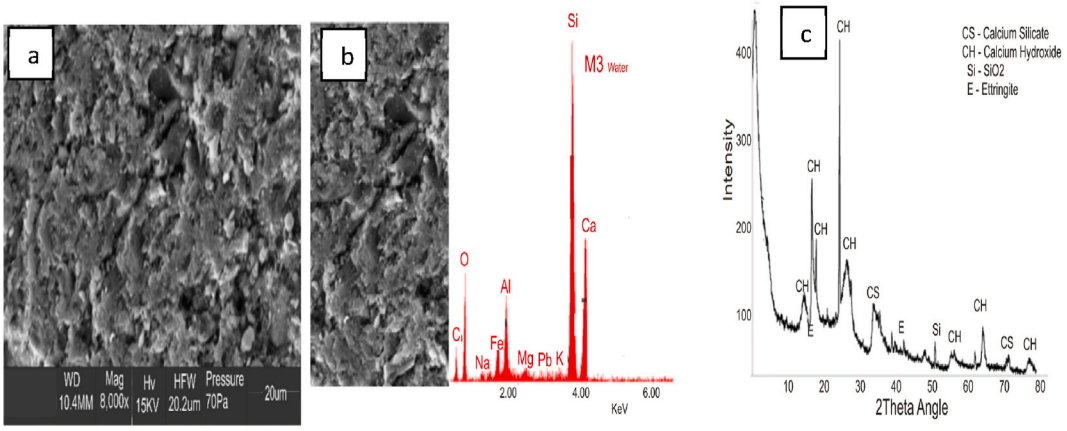

Fig. 10. Microstructural properties of G60C40 (a) SEM (b) EDX (c) XRD

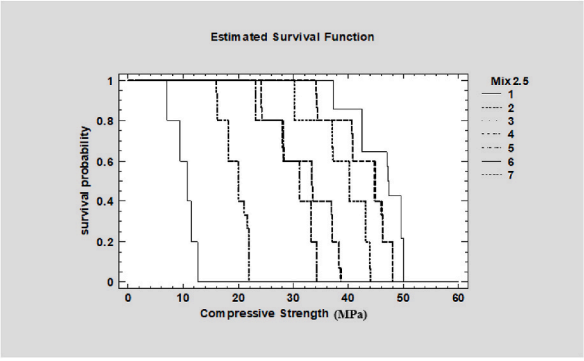

Fig. 11. Survival probability of GPC

composition and above perform better than conventional concrete of the same mix and this is further supported by the findings of Preethi, Sintha, Raj, Tamilarasan & Vinith [85]. The results obtained from the mechanical tests established G60C40 as the optimum mix in this study.

3.3. Microstructural analyses

Fig. 9 presents the SEM-EDX and XRD of the control experiment while Fig. 10 shows the SEM-EDX of the G60C40 sample.

The image of the internal structure of the conventional concrete that was produced at 9000x as shown in Fig. 9, shows some internal cracks which could have developed from the stress caused in the structure during the crushing phase of the concrete [86]. The image reveals the presence of ettringite. The ettringite is a common mineral formed in concrete due to cement hydration [87]. The internal structure of G60C40 shown in Fig. 10 was produced at 8,000x magnification. The image revealed the bonding within the internal structure of the geopolymer concrete. According to Kallesten et al. [88], higher internal cohesion results in higher strength. The micro-cracks developed in the internal structure could develop due to the internal stresses that resulted from the crushing of the GPC samples as in the control [86]. The structure of G60C40 GPC also contains partially reacted particles as a result of the low reactivity of CBA when compared to GGBS. The higher the composition level of GGBS in the GPC structure, the higher the geopolymerization [89]. The EDX chart of the control experiment shown in Fig. 9b revealed high peaks of O and Ca. The high Ca content confirms the high Ca content revealed by the chemical composition of cement. The results from EDX analysis of the G60C40 show the presence of Si, Ca, Na, Al, and O. This established the formation of N-A-S-H gel and N-A-S-H gel, which exist together. The EDX result of the G60C40 GPC products further confirms the chemical composition of the constituent materials. The SiO_2 composition level in natural sand is above 60% and about 20% in the mixture of NaOH and Na_2SiO_3 while it is about 30% in NaOH [90] and above 60% in gravel [91]. The presence of SiO_2 in GGBS, CBA, sand, gravel, and Na_2SiO_3 explains the reason for the dominant composition of Si revealed in the EDX results of G60C40.

The XRD pattern of the control experiment in Fig. 9c shows several humps of calcium silicate, calcium hydroxide, silica, and ettringite between $2\Theta = 10$ and $2\Theta = 80$. The Ettringite revealed in the XRD pattern of the control sample confirms the ettringite shown in the SEM image of the control sample. The humps, calcium silicate, calcium hydroxide, and silica as observed in the XRD pattern of the G60C40 GPC shown in Fig. 10c were between $2\Theta = 20$ and $2\Theta = 70$. The quartz formed in the G60C40 GPC sample is more intense because of the matrix of sand particles [92]. The broad humps seen in the pattern of the geopolymer matrix establish the

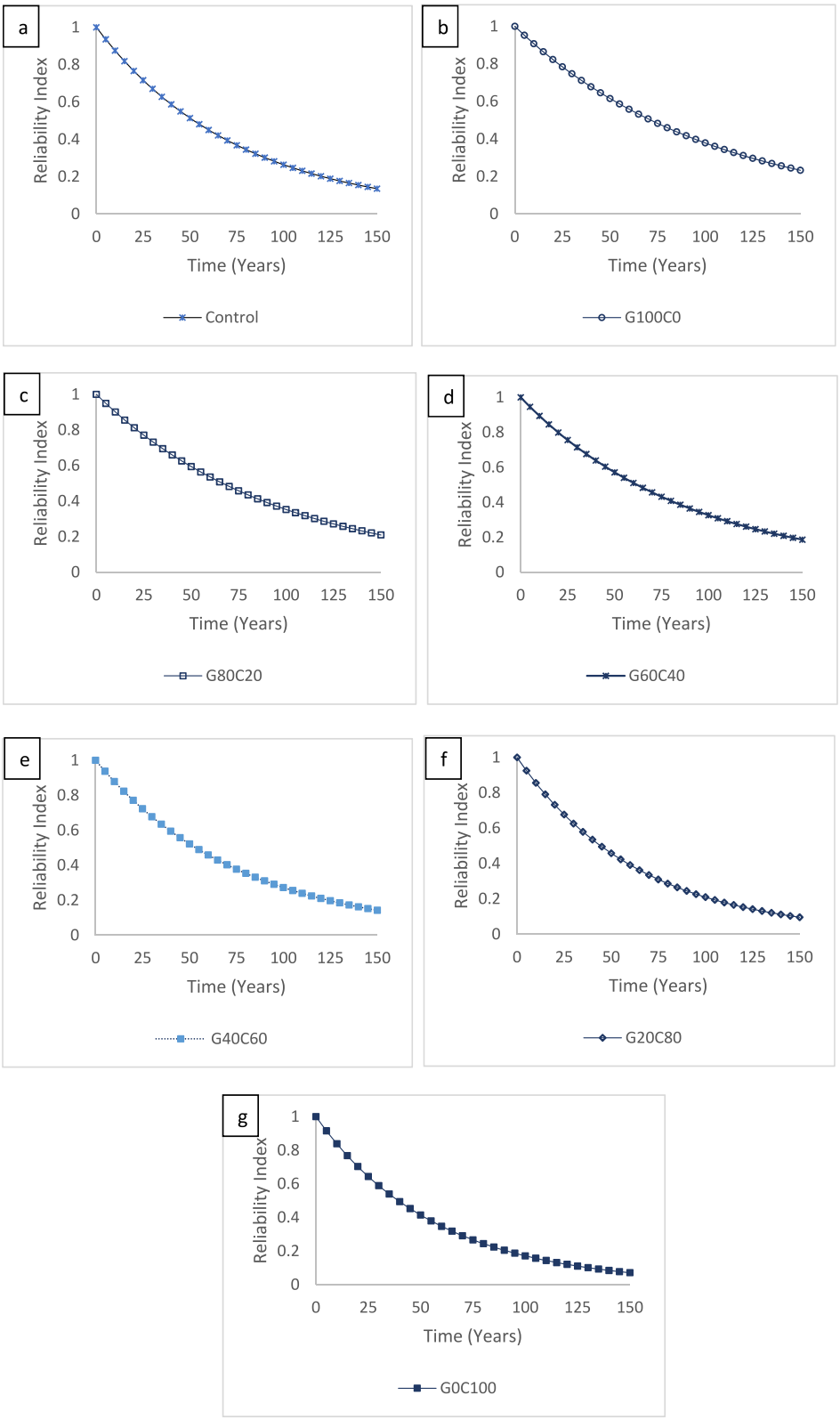

Fig. 12. Reliability index.

formation of amorphous geopolymer matrixes [93].

3.4. Reliability of GPC

The lines labeled 1,2,3,4,5,6 and 7 denote G100C0, G80C20, G60C40, G40C60, G20C80, G0C100 and control respectively in Fig. 11. G100C0 is revealed to have the highest survival probability. The survival probability of the GPC reduced from G100C0 to G0C100. The survival probability of G100C0, G80C20, and G60C40 are higher than the survival probability of conventional concrete. Nevertheless, the survival probability of G40C60, G20C80, and G0C100 is lower than that of the control experiment. The reliability indexes established for the GPC and the conventional concrete are shown in Fig. 12 (a)-(g).

G100C0 exhibited a satisfactory level of reliability up to 65 years of operation while the G80C20 exhibited a satisfactory level of reliability within operation life that is greater than 60 years but less than 65 years. Meanwhile, G60C40 exhibited a satisfactory level of reliability within an operation period beyond 55 years but less than 60 years while the G40C60 exhibited a satisfactory level of reliability within an operation period of 50 years. G20C80 exhibited a satisfactory level of reliability within the years of operation beyond 40 years but less than 45 years of operation while G0C100 exhibited a satisfactory level of reliability within operation time beyond 35 years but less than 40 years of operation. Based on the expected 50 years of service life of structures, G100C0, G80C20, G60C40, and G40C60 GPC are reliable for up to 50 years of service life of structures. Similarly, the trend observed in the study of Ibrahim et al. [94] where the constant failure rate method was used to assess the reliability of heated rubber tyre concrete, agrees with the findings in this study. Reliability assessments relate practical approaches to verify the safety of designs that are used in fields of engineering by establishing relationships between uncertainties that influence the degree of safety of a structure. It also evaluates the relationship between uncertain parameters that affect design parameters and performance measures. When a reliability assessment is carried out, a reliability index (β) that helps to make safe-level decisions is established [95].

4. Conclusion

Having successfully carried out reliability analyses of GPC developed using GGBS and CBA, the following conclusions are drawn:

i. The combination of GGBS and CBA can be utilized as supplementary materials to produce GPC. Nevertheless, the strength of the GPC depends on the ratio of the combination. To produce GPC with higher strength compared to conventional concrete of the same mix, GGBS content should be $\geq$ 60% and the CBA content should be $\leq$ 40%.
ii. The density of GGBS and CBA-based GPC is lower than the density of conventional concrete.
iii. The strength of the GPC increases with an increase in GGBS composition and curing period, and it decreases with an increase in CBA composition. Meanwhile, the rate of strength development of the GPC decreases after 28 days of curing and with an increase in CBA composition.
iv. GPC is reliable for satisfactory performance up to the expected 50 years of service life of structures.

Author statement

John Oluwafemi: Conceptualization, Methodology, Original draft preparation, Experimentation.
Justin Lazarus.: Data curation, Experimentation.
Adeola Adedeji: Supervision.
Olatokunbo Ofuyatan: Supervision, Validation.
Deborah Bankole: Analysis.
Adeola Adedeji: Reviewing and Editing.

Declaration of competing interest

The authors declare that they have no known competing financial interests or personal relationships that could have appeared to influence the work reported in this paper.

Data availability

Data will be made available on request.

Acknowledgment

The authors acknowledge Covenant University for providing an enabling environment for this research. The authors also acknowledge Master Builders Construction Chemicals Solutions Nigeria Limited, African Refractory and Allied Products Limited, and Lafarge for providing superplasticizer, steel slag, and chemical composition analyses respectively.

References

[1] E. Ikponmwosa, S. Ehikhuenmen, The effect of ceramic waste as coarse aggregate on strength properties of concrete, Niger. J. Technol. 36 (3) (Jun. 2017) 691–696, https://doi.org/10.4314/NJT.V36I3.5.

[2] P. Saranya, P. Nagarajan, A.P. Shashikala, Eco-friendly GGBS Concrete: a State-of-The-Art Review Investigating the influence of cement replacement by high volume of GGBS and PFA on the mechanical performance of cement mortar Eco-friendly GGBS Concrete: a State-of-The-Art Review, in: IOP Conference Series: Materials Science and Engineering, vol. 330, 2018, pp. 1–6, https://doi.org/10.1088/1757-899X/330/1/012057.

[3] S. Salehi, J. Khattak, F.K. Saleh, S. Igbojekwe, Investigation of mix design and properties of geopolymers for application as wellbore cement, J. Pet. Sci. Eng. 178 (Jul. 2019) 133–139, https://doi.org/10.1016/J.PETROL.2019.03.031.

[4] M. Wasim, T. Duc, D. Law, A state-of-the-art review on the durability of geopolymer concrete for sustainable structures and infrastructure, Construct. Build. Mater. 291 (2021), 123381, https://doi.org/10.1016/j.conbuildmat.2021.123381.

[5] F. Hannanee, et al., Geopolymer as underwater concreting material : a review, Construct. Build. Mater. 291 (2021), 123276, https://doi.org/10.1016/j.conbuildmat.2021.123276.

[6] K. Chen, D. Wu, L. Xia, Q. Cai, Z. Zhang, Geopolymer concrete durability subjected to aggressive environments - a review of influence factors and comparison with ordinary Portland cement, Construct. Build. Mater. 279 (2021), 122496, https://doi.org/10.1016/j.conbuildmat.2021.122496.

[7] J. Davidovits, Geopolymer cement a review, Geopolymer Sci. Tech. (2013) 1–11.

[8] N.H.A. Lim, et al., Effect of curing conditions on compressive strength of FA-POFA-based geopolymer mortar, IOP Conf. Ser. Mater. Sci. Eng. 431 (9) (Oct. 2018), 092007, https://doi.org/10.1088/1757-899X/431/9/092007.

[9] Saloni, et al., Performance of rice husk Ash-Based sustainable geopolymer concrete with Ultra-Fine slag and Corn cob ash, Construct. Build. Mater. 279 (Apr. 2021), 122526, https://doi.org/10.1016/J.CONBUILDMAT.2021.122526.

[10] F. Farooq, et al., Geopolymer concrete as sustainable material : a state of the art review, Construct. Build. Mater. 306 (September) (2021), 124762, https://doi.org/10.1016/j.conbuildmat.2021.124762.

[11] M. Amran, S. Huang, S. Debbarma, R.S.M. Rashid, Fire resistance of geopolymer concrete : a critical review, Construct. Build. Mater. 324 (January) (2022), 126722, https://doi.org/10.1016/j.conbuildmat.2022.126722.

[12] J. Alex, J. Dhanalakshmi, B. Ambedkar, Experimental investigation on rice husk ash as cement replacement on concrete production, Construct. Build. Mater. 127 (Nov. 2016) 353–362, https://doi.org/10.1016/J.CONBUILDMAT.2016.09.150.

[13] C.A. Fapohunda, B.A. Adigo, B.I. Famodimu, Splitting tensile strength and compressive strength ratios and relations for concrete made with different grades of Nigerian Portland limestone cement (plc), FUW Trends Sci. Technol. Journal 5 (3) (2020) 802–808. www.ftstjournal.com e-ISSN.

[14] Shashikant, G. Prince Arulraj, A research article on Geopolymer concrete, Int. J. Innovative Technol. Explor. Eng. 8 (9 Special Issue 2) (2019) 499–502, https://doi.org/10.35940/ijitee.I1106.0789S219.

[15] A. Hassan, M. Arif, M. Shariq, Influence of microstructure of geopolymer concrete on its mechanical properties-A review, Lect. Notes Civ. Eng. 35 (2020) 119–129, https://doi.org/10.1007/978-981-13-7480-7_10.

[16] T. Whitehead, Geopolymer Concrete, A Carbon-Neutral Alternative to Cement, *Beyond Cement*: Geopolymer Concrete, 2017. https://www.the-possible.com/geopolymer-concrete-carbon-neutral-alternative-to-cement/. (Accessed 28 May 2022).

[17] A.L. Almutairi, B.A. Tayeh, A. Adesina, H.F. Isleem, A.M. Zeyad, Potential applications of geopolymer concrete in construction: a review, Case Stud. Constr. Mater. 15 (Dec. 2021), e00733, https://doi.org/10.1016/J.CSCM.2021.E00733.

[18] X. Hua, J.L. Provis, J.S.J. Van Deventer, P.V. Krivenko, Characterization of aged slag concretes, Materials J. 105 (2) (Mar. 2008) 131–139, https://doi.org/10.14359/19753.

[19] C. Burne, Green Concrete Proves More Durable to Fire, Phys.org, 2015. https://phys.org/news/2015-06-green-concrete-durable.html. (Accessed 28 May 2022).

[20] P. Zhang, L. Kang, Y. Zheng, T. Zhang, B. Zhang, Influence of SiO2/Na2O molar ratio on mechanical properties and durability of metakaolin-fly ash blend alkali-activated sustainable mortar incorporating manufactured sand, J. Mater. Res. Technol. 18 (May 2022) 3553–3563, https://doi.org/10.1016/J.JMRT.2022.04.041.

[21] P. Zhang, X. Han, S. Hu, J. Wang, T. Wang, High-temperature behavior of polyvinyl alcohol fiber-reinforced metakaolin/fly ash-based geopolymer mortar, Compos. B Eng. 244 (Sep. 2022), 110171, https://doi.org/10.1016/J.COMPOSITESB.2022.110171.

[22] G. Jayarajan, S. Arivalagan, An experimental studies of geopolymer concrete incorporated with fly-ash & GGBS, Mater. Today Proc. 45 (Jan. 2021) 6915–6920, https://doi.org/10.1016/J.MATPR.2021.01.285.

[23] T. Revathi, R. Jeyalakshmi, Fly ash GGBS geopolymer in boron environment: a study on rheology and microstructure by ATR FT-IR and MAS NMR, Construct. Build. Mater. 267 (Jan. 2021), 120965, https://doi.org/10.1016/J.CONBUILDMAT.2020.120965.

[24] D.A. Salas, A.D. Ramirez, N. Ulloa, H. Baykara, A.J. Boero, Life cycle assessment of geopolymer concrete, Construct. Build. Mater. 190 (Nov. 2018) 170–177, https://doi.org/10.1016/J.CONBUILDMAT.2018.09.123.

[25] X. Jiang, R. Xiao, M. Zhang, W. Hu, Y. Bai, B. Huang, A laboratory investigation of steel to fly ash-based geopolymer paste bonding behavior after exposure to elevated temperatures, Construct. Build. Mater. 254 (Sep. 2020), 119267, https://doi.org/10.1016/J.CONBUILDMAT.2020.119267.

[26] A.E. Kurtoglu, et al., Advances in concrete construction, Adv. Concr. Constr. 6 (4) (Aug. 2018) 345, https://doi.org/10.12989/ACC.2018.6.4.345.

[27] S. Luhar, I. Luhar, R. Gupta, Durability performance evaluation of green geopolymer concrete. https://doi.org/10.1080/19648189.2020.1847691, 2020 doi: 10.1080/19648189.2020.1847691.

[28] V. Ramesh, K. Srikanth, Mechanical properties and mix design of geopolymer, concrete-A review 184 (2020) 1–5, https://doi.org/10.1051/e3sconf/202018401091.

[29] C. Gunasekara, P. Atzarakis, W. Lokuge, D.W. Law, S. Setunge, Novel analytical method for mix design and performance prediction of high calcium fly ash geopolymer concrete, Polymer 13 (2021) 900, https://doi.org/10.3390/POLYM13060900, vol. 13, no. 6, p. 900, Mar. 2021.

[30] A. Barambu, O. Uche, M. Abdulwahab, Reliability-based code calibration for load and safety factors for the design of a simply supported steel beam, J. Res. Inf. Civ. Eng. 14 (2017) 1–17.

[31] D.N. Kolo, J.I. Aguwa, T.Y. Tsado, M. Abdullahi, A. Yusuf, S.F. Oritola, Reliability studies on reinforced concrete beam subjected to bending forces with natural stone as coarse aggregate, Asian J. Civ. Eng. 22 (3) (Apr. 2021) 485–491, https://doi.org/10.1007/S42107-020-00327-Y/FIGURES/8.

[32] M. Ghabdian, S.B.B. Aval, M. Noori, W.A. Altabey, Reliability of reinforced concrete beams in serviceability limit state via microprestress-solidification theory, Struct. Health Monitor. Strategy 236 (5) (Jan. 2022) 1077–1093, https://doi.org/10.1177/14644207211069035, doi: 10.1177/1464420721106903.

[33] E.G. Abdelouafi, K. Benaissa, K. Abdellatif, Reliability analysis of reinforced concrete buildings: comparison between FORM and ISM, Procedia Eng. 114 (Jan. 2015) 650–657, https://doi.org/10.1016/J.PROENG.2015.08.006.

[34] M. Ghanooni-Bagha, M.A. Shayanfar, O. Reza-Zadeh, M. Zabihi-Samani, The effect of materials on the reliability of reinforced concrete beams in normal and intense corrosions, Eksploat. i Niezawodn. 19 (3) (2017) 393–402, https://doi.org/10.17531/EIN.2017.3.10.

[35] O.J. Aladegboye, D.A. Opeyemi, O.D. Atoyebi, S.L. Akingbonmire, E.M. Ibitogbe, Reliability analysis of reinforced concrete beam using varying properties, IOP Conf. Ser. Earth Environ. Sci. 445 (1) (Feb. 2020), 012031, https://doi.org/10.1088/1755-1315/445/1/012031.

[36] R.T. Loto, A. Busari, Electrochemical study of the inhibition effect of cow bone ash on the corrosion resistance of mild steel in artificial concrete pore solution, Cogent Eng. 6 (1) (2019), https://doi.org/10.1080/23311916.2019.1644710.

[37] J.A. Bhat, R.A. Qasab, A.R. Dar, Machine Crushed Animal Bones as Partial Replacement of Coarse Aggregates in Lightweight Concrete, vol. 7, 2012 no. 9.

[38] Bs DOE, Department of Environment, 1988. UK.

[39] I. Pane Herwani, I. Imran, B. Budiono, Compressive strength of fly ash-based geopolymer concrete with a variable of sodium hydroxide (NaOH) solution molarity, MATEC Web Conf 147 (Jan. 2018), https://doi.org/10.1051/MATECCONF/201814701004.

[40] A. Kanagalakshmi, J. Vindhya, International journal of engineering research in mechanical and civil engineering, Int. J. Eng. Res. Mech. Civ. Eng. (2019) 1–4.

[41] J. Akinyele, A. Adekunle, O. Ogundaina, The effect of partial replacement of cement with bone ash and wood ash in concrete, Int. J. Eng. 14 (4) (2016) 199–204.

[42] J.O. Aweda, P.O. Omoniyi, I.O. Ohijeagbon, Suitability of pulverized cow bones as a paving tile constituent, IOP Conf. Ser. Mater. Sci. Eng. 413 (1) (Sep. 2018), 012046, https://doi.org/10.1088/1757-899X/413/1/012046.

[43] K. D. Oluborode and I. S. Ayeni, "Evaluation of compressive strength of concrete produced with cow bones as partial replacement for coarse aggregates," IOSR J. Mech. Civ. Eng. e-ISSN, vol. 16, no. 2, pp. 72–74, doi: 10.9790/1684-1602027274.

[44] A. Olutaiwo, Y. Olalekan, E. Ikechukwu, Utilizing cow bone ash (CBA) as partial replacement for cement in highway rigid pavement construction, Int. J. Civ. Eng. 5 (2) (Feb. 2018) 13–19, https://doi.org/10.14445/23488352/IJCE-V5I2P104.
[45] S.V. Patankar, Y.M. Ghugal, S.S. Jamkar, Effect of concentration of sodium hydroxide and degree of heat curing on fly ash-based geopolymer mortar, Indian J. Mater. Sci. 2014 (May 2014) 1–6, https://doi.org/10.1155/2014/938789.
[46] O.M. Okeyinka, F.A. Olutoge, L.O. Okunlola, Durability performance of cow-bone ash (CBA) blended cement concrete in aggressive environment, Int. J. Sci. Res. Publ. 8 (12) (Dec. 2018), https://doi.org/10.29322/IJSRP.8.12.2018.P8408.
[47] British Standard EN 12620, Aggregates from Natural Sources for Concrete, Br. Stand. Inst., 2013.
[48] J. Xie, J. Wang, R. Rao, C. Wang, C. Fang, Effects of combined usage of GGBS and fly ash on workability and mechanical properties of alkali activated geopolymer concrete with recycled aggregate, Compos. B Eng. 164 (May 2019) 179–190, https://doi.org/10.1016/J.COMPOSITESB.2018.11.067.
[49] B. Zhang, Y. Feng, J. Xie, D. Lai, T. Yu, D. Huang, Rubberized geopolymer concrete: dependence of mechanical properties and freeze-thaw resistance on replacement ratio of crumb rubber, Construct. Build. Mater. 310 (Dec. 2021), 125248, https://doi.org/10.1016/J.CONBUILDMAT.2021.125248.
[50] T.Y. Tsado, T.W.E. Adejumo, Y. Adamu, Performance Evaluation of Egg-Shells and Cow Bone Ashes as Pozzolana in Concrete Production, 2018, pp. 1–10.
[51] M. Abbass, D. Singh, G. Singh, Properties of hybrid geopolymer concrete prepared using rice husk ash, fly ash and GGBS with coconut fiber, Mater. Today Proc. 45 (Jan. 2021) 4964–4970, https://doi.org/10.1016/J.MATPR.2021.01.390.
[52] J. Dai, Q. Wang, C. Xie, Y. Xue, Y. Duan, X. Cui, The effect of fineness on the hydration activity index of ground granulated blast furnace slag, Materials 12 (18) (Sep. 2019), https://doi.org/10.3390/MA12182984.
[53] M. Ahsan, A. Dewan, S. Mustafi, S. Ahmed, Characterization of crystalline phases of bone ash, Bangladesh J. Sci. Ind. Res. 47 (3) (Dec. 2012) 265–268, https://doi.org/10.3329/BJSIR.V47I3.13057.
[54] R.A. Olaoye, O.D. Afolayan, K.A. Adeyemi, L.O. Ajisope, O.S. Adekunle, Adsorption of selected metals from cassava processing wastewater using cow-bone ash, Sci. African 10 (Nov. 2020), e00653, https://doi.org/10.1016/J.SCIAF.2020.E00653.
[55] I. Koren, C.M. Krishna, Hardware Fault Tolerance, Fault-Tolerant Syst., 2021, pp. 11–57, https://doi.org/10.1016/B978-0-12-818105-8.00012-7.
[56] M.A. Muhammad, B.K. Mohammed, F.R. Ahmed, B.S. Al Numan, Critical evaluation for grading and fineness modulus of concrete sands used in sulaymaniyah city-Iraq, J. Eng. 27 (10) (Oct. 2021) 34–49, https://doi.org/10.31026/J.ENG.2021.10.03.
[57] V. Ramesh, K. Srikanth, Mechanical properties and mix design of geopolymer concrete-A review, in: E3S Web of Conferences, 2021, pp. 1–5, https://doi.org/10.1051/e3sconf/202018401091.
[58] C. Jithendra, S. Elavenil, Role of superplasticizer on GGBS based geopolymer concrete under ambient curing, Mater. Today Proc. 18 (Jan. 2019) 148–154, https://doi.org/10.1016/J.MATPR.2019.06.288.
[59] P. Saranya, P. Nagarajan, A.P. Shashikala, Behaviour of GGBS-dolomite geopolymer concrete beam-column joints under monotonic loading, Structures 25 (Jun. 2020) 47–55, https://doi.org/10.1016/J.ISTRUC.2020.02.021.
[60] S. Oyebisi, A. Ede, F. Olutoge, B. Ngene, Assessment of activity indexes on the splitting tensile strengthening of geopolymer concrete incorporating supplementary cementitious materials, Mater. Today Commun. 24 (Sep. 2020), 101356, https://doi.org/10.1016/J.MTCOMM.2020.101356.
[61] N. Poornima, D. Katyal, T. Revathi, M. Sivasakthi, R. Jeyalakshmi, Effect of curing on mechanical strength and microstructure of fly ash blend GGBS geopolymer, Portland cement mortar and its behavior at elevated temperature, Mater. Today Proc. 47 (Jan. 2021) 863–870, https://doi.org/10.1016/J.MATPR.2021.04.087.
[62] S. Oyebisi, A. Ede, F. Olutoge, S. Ogbiye, Evaluation of reactivity indexes and durability properties of slag-based geopolymer concrete incorporating corn cob ash, Construct. Build. Mater. 258 (Oct. 2020), 119604, https://doi.org/10.1016/J.CONBUILDMAT.2020.119604.
[63] M. Venu, T.D. Gunneswara Rao, Tie-confinement aspects of fly ash-GGBS based geopolymer concrete short columns, Construct. Build. Mater. 151 (Oct. 2017) 28–35, https://doi.org/10.1016/J.CONBUILDMAT.2017.06.065.
[64] P. Kumar, C. Pankar, D. Manish, A.S. Santhi, Study of mechanical and microstructural properties of geopolymer concrete with GGBS and Metakaolin, Mater. Today Proc. 5 (14) (Jan. 2018) 28127–28135, https://doi.org/10.1016/J.MATPR.2018.10.054.
[65] B. Rajini, C. Sashidhar, Prediction mechanical properties of GGBS based on geopolymer concrete by using analytical method, Mater. Today Proc. 19 (Jan. 2019) 536–540, https://doi.org/10.1016/J.MATPR.2019.07.729.
[66] J. Wang, J. Xie, C. Wang, J. Zhao, F. Liu, C. Fang, Study on the optimum initial curing condition for fly ash and GGBS based geopolymer recycled aggregate concrete, Construct. Build. Mater. 247 (Jun. 2020) 118540, https://doi.org/10.1016/J.CONBUILDMAT.2020.118540.
[67] S. Oyebisi, A. Ede, F. Olutoge, D. Omole, Geopolymer concrete incorporating agro-industrial wastes: effects on mechanical properties, microstructural behaviour and mineralogical phases, Construct. Build. Mater. 256 (Sep. 2020) 119390, https://doi.org/10.1016/J.CONBUILDMAT.2020.119390.
[68] A. Olutaiwo, Y. Olalekan, E. Ikechukwu, Utilizing cow bone ash (CBA) as partial replacement for cement in highway rigid pavement construction, SSRG Int. J. Civ. Eng. 5 (2018).
[69] British Standard EN 12350-2, Testing Fresh Concrete: Method for Determination of Slump, Br. Stand. Inst., 2009.
[70] British Standard EN 12350-4, Testing Fresh Concrete: Method for Determination of Compacting Factor, Br. Stand. Inst., 2009.
[71] British Standard 1881-125, Testing Concrete Methods for Mixing and Sampling Fresh Concrete in the Laboratory, Br. Stand. Inst., 2013.
[72] British Standard EN 12390 -2, Testing Hardened Concrete: Making and Curing Specimens for Strength Tests, Br. Stand. Inst., 2009.
[73] British Standard EN 12390- 7, Testing Hardened Concrete: Density of Hardened Concrete, Br. Stand. Inst., 2009.
[74] British Standard EN 12390- 3, Testing Hardened Concrete: Compressive Strength of Test Specimens, Br. Stand. Inst., 2009.
[75] British Standard EN 12390- 6, Testing Hardened Concrete: Tensile Splitting Strength of Test Specimens, Br. Stand. Inst., 2013.
[76] British Standard EN 12390 -5, Testing Hardened Concrete: Flexural Strength of Test Specimens, Br. Stand. Inst., 2009.
[77] P. Pougnet, F. Bayle, H. Maanane, P.R. Dahoo, Reliability prediction of embedded electronic systems: the FIDES guide, Embed. Mechatron. Syst. Anal. Fail. Predict. Reliab. (Jan. 2019) 189–216, https://doi.org/10.1016/B978-1-78548-189-5.50008-2.
[78] S. Getahun, B. Bewket, Journal of Civil & Environmental Engineering A Study on Effect of Partial Replacement of Cement by Cattle Bone Ash in Concrete Property, 2021.
[79] L.I. O, O.R. O, M.K. A, A.M. O, Evaluation of Rice Husk Ash and Bone Ash Mixed as Partial Replacement of Cement in Concrete, Corpus 2 (34) (2017) 258–264.
[80] M. Zuaiter, et al., Properties of slag-fly ash blended geopolymer concrete reinforced with hybrid glass fibers, Buildings 12 (8) (Jul. 2022) 1114, https://doi.org/10.3390/BUILDINGS12081114.
[81] R.M. Waqas, F. Butt, X. Zhu, T. Jiang, R.F. Tufail, A comprehensive study on the factors affecting the workability and mechanical properties of ambient cured fly ash and slag based geopolymer concrete, Appl. Sci. 11 (2021) 8722, https://doi.org/10.3390/APP11188722, vol. 11, no. 18, p. 8722, Sep. 2021.
[82] A. Shobha, D. Hadole, Properties of fly ash based geopolymer concrete with GGBS & RHA, Int. J. Eng. Res. Technol. 10 (5) (May 2021), https://doi.org/10.17577/IJERTV10IS050188.
[83] G. Rao, B. Kumar, Experimental investigation of GGBS based geopolymer concrete with steel fibers, Int. J. Recent Technol. Eng. 7 (6) (2019) 49–55.
[84] S.M.A. Kabir, U.J. Alengaram, M.Z. Jumaat, A. Sharmin, A. Islam, Influence of molarity and chemical composition on the development of compressive strength in POFA based geopolymer mortar, Adv. Mater. Sci. Eng. 2015 (2015), https://doi.org/10.1155/2015/647071.
[85] P. Preethi, N. Sintha, M. Prithivi Raj, K. Tamilarasan, R. Vinith, Exploration on geopolymer concrete using GGBS and silica fume, Mater. Today Proc. (Dec. 2020), https://doi.org/10.1016/J.MATPR.2020.10.768.
[86] A. Fernandez-Jimenez, I. García-Lodeiro, A. Palomo, Durability of alkali-activated fly ash cementitious materials, J. Mater. Sci. 42 (9) (Dec. 2006) 3055–3065, https://doi.org/10.1007/S10853-006-0584-8, 2006 429.
[87] S. Tao, Y. Yumei, Quantitative analysis of ettringite formed in the hydration, Products of high-alite cements 27 (9) (Sep. 2015) 497–505, https://doi.org/10.1680/adcr.14.00054, doi: 10.1680/ADCR.14.00054.
[88] B. Kallesten, S. Kakay, K. Gebremariam, Synthesis and characterization of fly ash and slag based geopolymer concrete, IOP Conf. Ser. Mater. Sci. Eng. 700 (1) (Nov. 2019), 012032, https://doi.org/10.1088/1757-899X/700/1/012032.

[89] J. Wang, W. Zheng, Y. Zhao, X. Zhang, Prediction of concrete failure time based on statistical properties of compressive strength, Appl. Sci. 10 (3) (Feb. 2020) 1–20, https://doi.org/10.3390/APP10030815.
[90] H. El-Hassan, N. Ismail, S. Al Hinaii, A. Alshehhi, N. Al Ashkar, Effect of GGBS and curing temperature on microstructure characteristics of lightweight geopolymer concrete, MATEC Web Conf 120 (Aug. 2017), https://doi.org/10.1051/MATECCONF/201712003004.
[91] A. Makani, T. Vidal, G. Pons, G. Escadeillas, Time-dependent behaviour of high performance concrete: influence of coarse aggregate characteristics, EPJ Web Conf. 6 (Jun. 2010), 03002, https://doi.org/10.1051/EPJCONF/20100603002.
[92] A. Blash, V. Lakshmi, Effect of fly ash on ground-granulated blast- furnace slag based geopolymer concrete, in: NIER International Conference, 2018, pp. 56–63.
[93] Z. Li, S. Liu, Influence of slag as additive on compressive strength of fly ash-based geopolymer, J. Mater. Civ. Eng. 19 (6) (Jun. 2007) 470–474, https://doi.org/10.1061/(ASCE)0899-1561(2007)19:6(470).
[94] O. Ibrahim, M. Usman, K. Okeke, F. Adeyemi, S. Ibrahim, Reliability assessment of heated rubber tyre concrete, J. Multidiscip. Eng. Sci. Stud. 7 (4) (2021).
[95] R. Aghamohammadi, K. Nasrollahzadeh, A. Mofidi, P. Gosling, Reliability-based assessment of bond strength models for near-surface mounted FRP bars and strips to concrete, Compos. Struct. 272 (Sep. 2021), 114132, https://doi.org/10.1016/J.COMPSTRUCT.2021.114132.